15. Trettin, U. Wechselwirkung von Enantiomeren in unverdünnten Flüssigkeiten. Thesis, Univ. Tübingen (1993).
16. Schurig, V. Enantiomer analysis by complexation GC: scope, merits, limitations. *J. Chromatogr.* **441,** 135–153 (1988).
17. Meinwald, J. *et al.* Inhalational anesthetics stereochemistry: Optical resolution of halothane, enflurane and isoflurane. *Science* **251,** 560–561 (1991).
18. Koppenhoefer, B. & Bayer, E. Chiral recognition in the resolution of enantiomers by GLC. *Chromatographia* **19,** 123–130 (1984).
19. König, W. A. Separation of enantiomers by capillary GC with chiral stationary phases *J. High Resolut. Chromatogr. Chromatogr. Commun.* **5,** 588–595 (1982).
20. Kubo, Y., Maeda, S., Tokita, S. & Kubo, M. Colorimetric chiral recognition by a molecular sensor. *Nature* **382,** 522–524 (1996).
21. James, T. D., Sandanayake, K. R. A. S. & Shinkai, S. Chiral discrimination of monosaccharides using a fluorescent molecular sensor. *Nature* **374,** 345–347 (1995).
22. Ide, J., Nakamoto, T. & Moriizumi, T. Discrimination of aromatic optical isomers using quartz resonator sensors. *Sens. Actuators A* **49,** 73–78 (1995).
23. Sauerbrey, G. Verwendung von Schwingquarzen zur Wägung dünner Schichten und zur Mikrowägung. *Z. Phys.* **155,** 206–222 (1959).

Acknowledgements. We thank H.-G. Brendle, R. Schlunk and B. Christian at the Institute of Organic Chemistry of the University of Tübingen for providing the enantioselective polymers and the chiral analyte N-TFA-Ala-OMe. This work was supported by the Deutsche Forschungsgemeinschaft.

Correspondence and requests for materials should be addressed to W.G. (e-mail: wg@ipc.uni-tuebingen.de).

A biosensor that uses ion-channel switches

B. A. Cornell, V. L. B. Braach-Maksvytis, L. G. King, P. D. J. Osman, B. Raguse, L. Wieczorek & R. J. Pace*

Co-operative Research Centre for Molecular Engineering & Technology, 126 Greville Street, Chatswood NSW 2067, Australia

Biosensors are molecular sensors that combine a biological recognition mechanism with a physical transduction technique. They provide a new class of inexpensive, portable instrument that permit sophisticated analytical measurements to be undertaken rapidly at decentralized locations[1]. However, the adoption of biosensors for practical applications other than the measurement of blood glucose is currently limited by the expense, insensitivity and inflexibility of the available transduction methods. Here we describe the development of a biosensing technique in which the conductance of a population of molecular ion channels is switched by the recognition event. The approach mimics biological sensory functions[2,3] and can be used with most types of receptor, including antibodies and nucleotides. The technique is very flexible and even in its simplest form it is sensitive to picomolar concentrations of proteins. The sensor is essentially an impedance element whose dimensions can readily be reduced to become an integral component of a microelectronic circuit. It may be used in a wide range of applications and in complex media, including blood. These uses might include cell typing, the detection of large proteins, viruses, antibodies, DNA, electrolytes, drugs, pesticides and other low-molecular-weight compounds.

The active elements of the ion-channel switch comprise a gold electrode to which is tethered a lipid membrane containing gramicidin ion channels[4] linked to antibodies. The molecular structure of the tethered membrane[5–14] results in an ionic reservoir[15] being formed between the gold electrode and the membrane. The ionic reservoir can be accessed electrically through connection to the gold electrode. In the presence of an applied potential, ions flow between the reservoir and the external solution when the channels are conductive. The ion current is switched off when mobile channels diffusing within the outer half of the membrane become crosslinked to antibodies immobilized at the membrane surface. This prevents them forming dimers with channels immobilized within the inner half of the membrane. The number of dimers is measured from the electrical conduction of the membrane. The switch has a high gain; a single channel facilitates the flux of up to a million ions per second. A quantitative model of the biosensor has been verified experimentally; see Supplementary Information.

The detection of analytes possessing multiple recognition sites is performed using the structure shown schematically in Fig. 1a. This structure is assembled using a combination of sulphur–gold chemistry and physisorption as described in Fig. 1 legend. The membrane consists of lipids and channels, some immobilized on the gold surface and some diffusing laterally within the plane of the membrane. The antibodies on the mobile channels scan an area of the order of 1 μm^2 in less than 5 minutes. Thus with a low density of channels and a high density of immobilized antibodies, each channel can access up to 10^3 more capture antibodies than if the gating mechanism were triggered by a directing binding of analyte to the channels. The speed and sensitivity of the biosensor response may be adjusted in direct proportion to the number of binding sites accessible to each mobile channel. This allows for quantitative detection of analyte from sub-picomolar to micromolar concentrations in less than 10 minutes.

The immobilized membrane components are shown in Fig. 2a. These compounds possess common sulphur and reservoir-forming segments. A fraction of the tethered species are hydrophilic spacer molecules, provided to increase the volume within the reservoir and to improve the conductivity of the membrane. Tethered membrane-spanning lipids are included to improve the stability of the membrane. This is reminiscent of the role played by membrane-spanning lipids found in archaebacteria[16]. These bacteria can survive at temperatures in excess of 100 °C. Tethering a substantial fraction of the lipid both stabilizes the lamella phase necessary for the formation of the membrane and inhibits the insertion of further material following the membrane assembly. Tethered membranes formed in this manner are stable over many months. A fraction of the membrane-spanning lipid is coupled to antibodies. This is the immobilized population of antibodies necessary for the switch function. The mobile membrane-forming species are shown in Fig. 2b.

A competitive version of the switch has been assembled and demonstrated for the detection of small analytes with only a single epitopic site. This is shown schematically in Fig. 1b.

Figure 2 Components used in the ICS biosensor assembly. **a**, The immobilized components of the membrane consist of a mixture of tethered gramicidin, gAYYSSB$_n$ (G_T), double-length reservoir half-membrane-spanning phytanyl lipids, (DLP), and full-membrane-spanning lipids, (MSL). The surface density of these tethered species is controlled by dilution with a low-molecular-weight hydrophilic spacer, mercaptoacetic acid disulphide MAAD or ethylene disulphide (EDS). A fraction of the tethered membrane spanning lipid, MSL_α, is biotinylated for subsequent coupling to streptavidin and an antibody fragment. These compounds are based on a common benzyl disulphide attachment moiety and an ethylene glycol chain. The thickness of the reservoir region is determined by the length (~4 nm) of the ethylene glycol chain segment. **b**, The main mobile component is a 30:70 (mole ratio) mix of glycerodiphytanylether (GDPE):diphytanyl ether phosphatidylcholine (DPEPC), which is mixed with a small fraction of mobile ion channels (G_α). For large analyte detection, the channel species employed is gA5XB. The biotinylation site on gA5XB is used for subsequent coupling to streptavidin and an antibody fragment. For small analyte detection, the mobile channel is the hapten-linked gA4Xdig.

* Permanent address: Chemistry Department, Faculty of Science, Australian National University, Canberra, ACT, Australia.

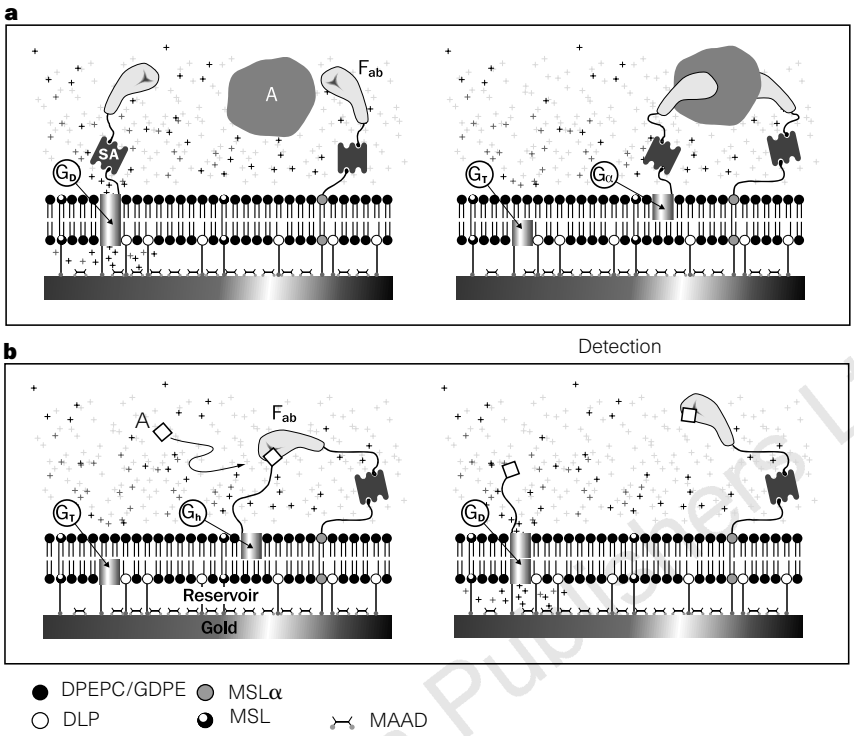

Figure 1 Schematic ion-channel switch (ICS) biosensor. **a**, Two-site sandwich assay. Immobilized ion channels (G_T), synthetic archaebacterial membrane-spanning lipids (MSL) and half-membrane-spanning tethered lipids (DLP) are attached to a gold surface via polar linkers and sulphur–gold bonds. Polar spacer molecules, (MAAD), are directly attached to the gold surface using the same chemistry. Mobile half-membrane-spanning lipids (DPEPC/GDPE) and mobile ion channels (G_α) complete the membrane. (Abbreviations are defined in Fig. 2 legend.) The mobile ion channels are biotinylated and coupled to biotinylated antibody fragments (Fab′) using streptavidin (SA) intermediates. Some of the membrane spanning lipids (MSL_α) possess biotin-tethered Fab′. In the absence of analyte (A), the mobile ion channels diffuse within the outer monolayer of the tethered membrane, intermittently forming conducting dimers (G_D). The addition of the targeted analyte crosslinks the Fabs on the MSL_α and G_α and forms complexes that tether the G_α distant from their immobilized inner-layer partners. This prevents the formation of channel dimers and lowers the electrical conductivity of the membrane. **b**, Competitive assay. Here a similar membrane is formed except that it contains hapten-linked gramicidin, (G_h). The membrane is rinsed with a streptavidin solution after which an appropriate biotinylated, hapten-specific Fab′ is added, forming complexes between the MSL_α and the G_h. The G_h is thus tethered distant from its immobilized inner-layer partners, G_T, preventing the formation of dimers and lowering the electrical conductance of the membrane. The sensor is stored in this state until the addition of analyte competes with the hapten for the Fab′, liberating the channel and resulting in an increase in the membrane conductance.

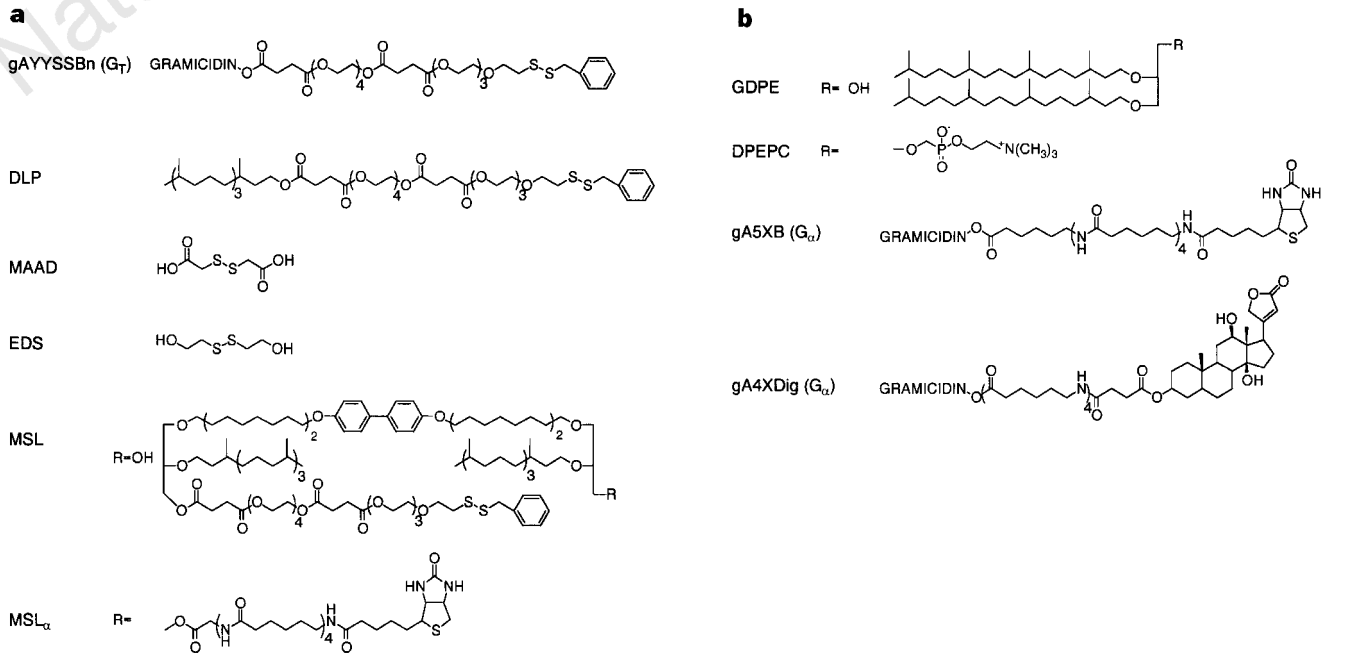

The ion-channel switch (ICS) biosensor requires none of the washing or reagent additions of the enzyme-linked immunosorbent assay (ELISA). This is a consequence of the capture and reporter antibodies being preassembled at the membrane surface. From the phase relationship between the excitation potential and the current flow we derive the admittance at minimum phase, $Y_{\phi min}$. For large, multiply bound analytes the sensor response is determined from the maximum rate of change of admittance (see Supplementary Information), $-(dY_{\phi min}/dt)_{max}$, which can be shown by numerical simulation to be a linear function of the concentration of analyte over more than six decades of detectable admittance change. The maximum slope can typically be attained after only 10% change in $Y_{\phi min}$ and provides ~3–4 decades of dynamic range for each 2 decades of variation of the initial $Y_{\phi min}$.

The response of the ICS biosensor to large analytes may be demonstrated using thyroid-stimulating hormone, TSH (relative molecular mass 28,000, M_r 28K). TSH comprises an α and β subunit to which it is possible to bind complementary Fabs (antigen-binding fragments of an antibody). To switch off the ion channels through crosslinking, a matched pair of antibodies is used, each one sensitive to one of the non-overlapping binding sites on the TSH. The response is shown in Fig. 3. If the membrane surface is prepared exclusively with biotinylated anti-ferritin Fab′, anti-α-TSH Fab′ or anti-β-TSH Fab′, the addition of TSH results in a small or negligible change in admittance. If however, an equal mixture of biotinylated anti-α-TSH *and* anti-β-TSH Fab′ is bound, the addition of TSH elicits a dramatic reduction in membrane admittance. The dependence of the admittance response on the Fab′ composition is consistent with the proposed mechanism. All of the six differently targeted, complementary anti-TSH Fab′ fragments we have tested have functioned successfully in the ICS biosensor. Digoxin (M_r 781), demonstrates the response of the ICS biosensor to small analytes. The mobile channels carry a digoxin hapten as shown in Fig. 2b. In the absence of analyte, the mobile channels crosslink to the immobilized antibody fragments preventing the formation of dimers and turning off the membrane conductance. The introduction of analyte competes with the hapten for the binding site within the antbody fragment, liberating the channel

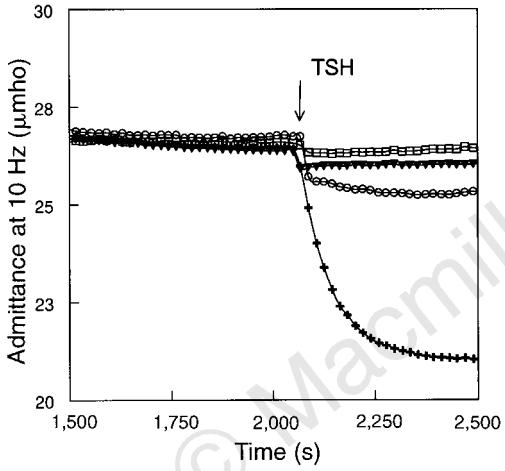

Figure 3 Response of ICS biosensor to TSH. **a**, Assembly procedures. First, a tethered membrane 0.16 mm^2 in area is formed on a freshly evaporated gold film. The gold film is 100 nm thick and is bonded to a clean glass microscope slide using a 5-nm layer of chromium. The slide is then immersed in an ethanol solution of the immobile lipid-layer mixture for 1 h at 20 °C. The mixture comprises 59 μM DLP, 4.4 nM MSL-4XB, 4.4 μM MSLOH, 7.5 nM gAYYSSB$_n$ and 35 μM EDS (see Fig. 2 legend for abbreviations). The slide is then removed and rinsed thoroughly in ethanol, air-dried, and clamped to a series of teflon cylinders, each 4 mm internal diameter, 5 mm long, each defining a well volume of 200 μl above the coated gold surface. A further 5 μl of mobile-layer mixture in ethanol solution is added, which contains 350 nM gA-5XB and a 14 mM (30 : 70) mix of GDPE : DPEPC, after which the slide is rinsed with ~500 μl of phosphate buffered saline (PBS). This induces the spontaneous formation of a bilayer membrane. Care is taken not to introduce air bubbles or to take the newly formed membrane surface through an air–water interface. Having rinsed three times with PBS to eliminate any residual excess membrane lipid, 5 μl of 1.6 μM streptavidin in PBS is added. Following incubation for 10 min, the supernatant is thoroughly rinsed with PBS and a further 20 μl of 0.2 μM b-Fab′ is added. This is then incubated for a further 10 min and thoroughly rinsed with PBS to remove residual material. The sensor is now stored ready to use. **b**, Measurement procedure. The admittance is measured at 10 Hz using an excitation amplitude of 50 mV and an offset potential of −300 mV at the gold electrode relative to the test solution. Traces are shown using different specificities of biotinylated Fab′: open squares, b-antiferritin; filled triangles, b-anti-α-TSH; circles, b-anti-β-TSH; and crosses, a 50 : 50 mix of b-anti-α-TSH and b-anti-β-TSH. 2 nM of TSH is added at the arrow. The mixed population of biotinylated anti-α and biotinylated anti-β Fab′ elicited a substantial response when the TSH was added. However, the other three biotinylated Fab′ populations only elicited a small or negligible response when used in isolation.

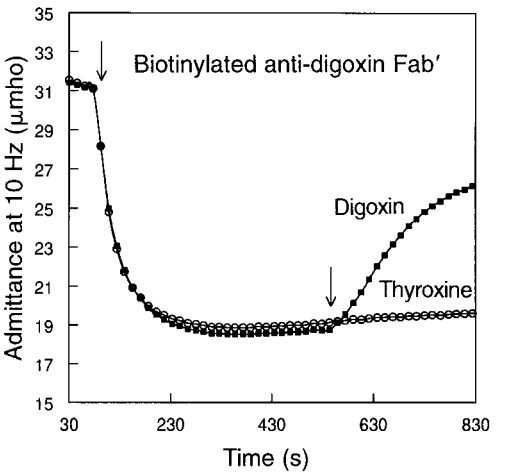

Figure 4 Response to digoxin. A similar membrane is prepared to that described in Fig. 3 legend. The principal difference is that the concentration of MSL_α is increased tenfold and G_α is replaced by G_h. The total concentration of MSL is maintained. Following the formation of the membrane, it is incubated with 40 nM streptavidin for 10 min and rinsed again. The addition of 5 μl of 50 nM biotinylated-antidigoxin (first arrow) results in a decrease in the admittance. The membrane is then thoroughly rinsed with PBS and stored ready for use. The addition of 3 μM (5 μl) digoxin (second arrow) causes the admittance to increase (filled squares). The rate and size of this increase is related to the concentration of digoxin. The process may be repeated many times following rinsing with PBS solution. A control is shown in which thyroxine was used in place of digoxin, eliciting no response (circles).

and increasing the conductance. An example of the formation of channel–Fab′ crosslinked species and their liberation upon the addition of digoxin is shown in Fig. 4. A control is also shown in which the addition of thyroxine fails to elicit a response. The absence of biotins on the lipid tether, the absence of the streptavidin linker or the correctly targeted Fab′ eliminates the response. A quantitative measure of analyte concentration may be obtained from either the absolute initial rate of admittance increase, or the equilibrium fractional admittance change (see Supplementary Information). These are essentially proportional to each other over the sensitivity range of the competitive assay. The range may be adjusted by varying the immobilised Fab′ surface density.

By varying the nature and type of receptor in the ICS biosensor, we have applied the technique to blood typing, the detection of bacteria, virus particles, DNA, drugs, antibodies and electrolytes. Receptors include antibodies, enzymes, DNA, binding proteins and synthetic ligands. The ion-transport properties of channels and ionophores other than gramicidin have also been studied[17,18]. For example, we have incorporated the K^+ ionophore valinomycin into a tethered membrane and successfully measured potassium concentration over physiologically relevant concentrations. The biosensor functions in human serum, plasma and whole blood. The biosensor may be assembled and measured on electrodes of dimensions from square centimetres to square micrometres. As the membrane area is decreased, the membrane leakage conductance decreases proportionally, but the conductance per channel remains constant. This means that with small electrodes (<30 μm diameter) it becomes possible to resolve the current transients associated with individual channels. Operation of the biosensor under these conditions of low channel density, coupled with the use of multi-electrode arrays of such membranes, promises to increase significantly the sensitivity of the device. □

Received 14 November 1996; accepted 14 April 1997

1. Scheller, F. W., Schubert, F. & Fedrowitz, J. (eds) *Frontiers in Biosensorics* Vols I & II (Birkhauser, Berlin, 1996).
2. Avrone, E. & Rospars, J. P. Modelling insect olfactory neurone signaling by a network utilising disinhibition. *Biosystems* **36,** 101–108 (1995).
3. Reiken, S. R. *et al*. Bispecific antibody modification of nicotine acetycholine receptors for biosensing. *Biosens. Bioelectron.* **11,** 91–102 (1996).
4. Koeppe, R. E. & Andersen, O. S. Engineering the gramicidin channel. *Annu. Rev. Biophys. Biomol. Struct.* **25,** 231–258 (1996).
5. McConnell, H. M., Watts, T. H., Weis, R. M. & Brian, A. A. Supported planar membranes in studies of cell-cell recognition in the immune system. *Biochim. Biophys. Acta* **864,** 95–106 (1986).
6. Florin, E.-L. & Gaub, H. E. Painted supported lipid membranes. *Biophys. J.* **64,** 375–383 (1993).
7. Lang, H., Duschl, C. & Vogel, H. A new class of thiolipids for the attachment of lipid bilayers on gold surfaces. *Langmuir* **10,** 197–210 (1994).
8. Steizle, M., Weismuller, G. & Sackmann, E. On the application of supported bilayers as receptive layers for biosensors with electrical detection. *J. Phys. Chem.* **97,** 2974–2981 (1993).
9. Plant, A. L., Gueguetchkeri, M. & Yap, W. Supported phospholipid/alkanethiol biomimetic membranes: insulating properties. *Biophys. J.* **67,** 1126–1133 (1994).
10. Folkers, J. P., Laibinis, P. E., Whitesides, G. M. & Deutch, J. Phase behaviour of two-component self-assembled monolayers of alkanethiolates on gold. *J. Phys. Chem.* **98,** 563–571 (1994).
11. Steinem, C., Janschoff, A., Ulrich, W. P., Sieber, M. & Galla, H. J. Impedance analysis of supported lipid bilayer membranes: a scrutiny of different preparation techniques. *Biochem. Biophys. Acta* **1279,** 169–180 (1996).
12. Lu, X. D., Ottova, A. L. & Tien, H. T. Biophysical aspects of agar-gel supported bilayer lipid membranes: a new method for forming and studying planar bilayer lipid membranes. *Bioelectrochem. Bioenerget.* **39,** 285–289 (1996).
13. Heysel, S., Vogel, H., Sanger, M. & Sigrist, H. Covalent attachment of functionalised lipid bilayers to planar waveguides for measuring protein binding to biomimetic membranes. *Protein Sci.* **4,** 2532–2544 (1995).
14. Rickert, J., Weiss, T., Kraas, W., Jung, G. & Gopel, W. A new affinity biosensor: self-assembled thiols as selective monolayer coatings of quartz crystal microbalances. *Biosens. Bioelectron.* **11,** 591–598 (1996).
15. Sackmann, E. Supported membranes: scientific and practical applications. *Science* **271,** 43–48 (1996).
16. Stetter, K. O. Hypothermophilic procaryotes. *FEMS Microbiol. Rev.* **18,** 149–158 (1996).
17. Hladky, S. B., Leung, J. C. H. & Fitzgerald, W. The mechanism of ion conduction by valinomycin-analysis of charge pulse responses. *Biophys. J.* **69,** 1758–1772 (1995).
18. Nikolelis, D., Siontorou, C. G., Krull, U. J. & Katrivanos, P. L. Ammonium ion minisensors from self-assembled bilayer lipid membranes using gramicidin as an ionophore. Modulation of ammonium selectivity by Platelet Activating Factor. *Anal. Chem.* **68,** 1735–1741 (1996).

Supplementary Information is available on *Nature*'s World-Wide Web site (http://www.nature.com) or as paper copy from Mary Sheehan at the London editorial office of *Nature*.

Acknowledgements. This work was supported by the Australian Industrial Research & Development Board and the Cooperative Research Centres (CRC) program. The partner organisations within the CRC for Molecular Engineering & Technology are the Commonwealth Scientific & Industrial Research Organisation, the University of Sydney and the Australian Membrane & Biotechnology Research Institute.

Correspondence and requests for materials should be addressed to B.A.C. (e-mail: bcornell@ambri.com.au).

Synthesis and X-ray structure of dumb-bell-shaped C_{120}

Guan-Wu Wang*, Koichi Komatsu*, Yasujiro Murata* & Motoo Shiro†

* *Institute for Chemical Research, Kyoto University, Uji, Kyoto 611, Japan*
† *Rigaku Corporation, 3-9-12 Matsubara-cho, Akishima, Tokyo 196, Japan*

The discovery and large-scale synthesis of fullerenes have aroused interdisciplinary interest in these closed-cage molecules[1–6]. C_{60} can be photopolymerized into a form in which the cages are thought to be linked by cyclic C_4 units in a [2 + 2] cycloaddition[7], provoking theoretical studies of the C_{60} dimer[8–15], the smallest subunit of such a polymer. The C_{60} dimers $C_{120}O$ (refs 16, 17), $C_{121}H_2$ (ref. 17) and $C_{120}O_2$ (ref. 18) have been reported, in which the two C_{60} molecules are linked by, respectively, a furan group, a cyclopentane ring and a cyclobutane ring plus two oxygen bridges; but the simplest dimer, C_{120} linked by a cyclobutane ring alone, has not so far been observed. We now report that this dumb-bell-shaped molecule can be synthesized by a solid-state mechanochemical reaction of C_{60} with potassium cyanide. Our X-ray structural analysis shows that the C_4 ring connecting the cages is square rather than rectangular—the latter is predicted theoretically[8,9,13–15]. The dimer dissociates cleanly into two C_{60} molecules on heating or one-electron reduction, but in the gas phase during mass-spectrometric measurements it undergoes successive loss of C_2 units, shrinking to even-numbered fullerenes such as C_{118} and C_{116} in a sequence similar to that seen for other large fullerenes[19,20].

Recently, we developed a new method to derivatize C_{60} in the solid state by the use of a 'vibrating mill'[21]. The key feature of this method is a high-speed vibration technique, which can activate the reaction system by bringing the reagents into very close contact at the preparative scale and by providing extra mechanical energy, much more effectively than the ball-milling technique[22]. The reaction of C_{60} with KCN in the solid state has led to the first preparation of dumb-bell-shaped C_{120} (**1**) instead of formation of $C_{60}H(CN)$ (**2**)[23] after quenching with trifluoroacetic acid.

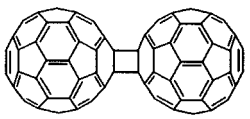

1

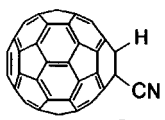

2

A mixture of C_{60} and 20 molar equivalents of KCN powder was vigorously vibrated for 30 min under nitrogen according to our previous procedure[21]. Analysis by high-performance liquid chromatography of the reaction mixture dissolved in *o*-dichlorobenzene (ODCB) on a Cosmosil Buckyprep column with toluene as the eluent showed only one major product besides unchanged C_{60}. Separation by flash chromatography on silica gel, eluted with hexane–toluene and then with toluene–ODCB, gave 70% of recovered C_{60} and 18% of C_{120} (**1**). Its structure was unequivocally determined as the [2 + 2] adduct of C_{60} based on the evidence shown below.

The product, isolated as a dark brown powder, has very low solubility in CS_2 and toluene, but is reasonably soluble (1–2 mg ml^{-1}) in ODCB. The ^{13}C NMR spectrum (Fig. 1) exhibited 15 signals (including one overlapped signal) in the sp^2 region and one signal at 76.22 p.p.m. in the sp^3 region, which are fully consistent with the assigned structure with D_{2h} symmetry. A comparison of the present data with the ^{13}C magic-angle spinning (MAS) NMR spectra of C_{60} polymers prepared under high pressure[24,25] has